THE UNIVERSITY OF
WARWICK

Original citation:
Fu, Y. (Ying), Romero, Maria, Habtemariam, Abraha, Snowden, Michael E., Song, Lijiang, Clarkson, Guy J., Qamar, Bushra, Pizarro, Ana M., Unwin, Patrick R. and Sadler, Peter J.. (2012) The contrasting chemical reactivity of potent isoelectronic iminopyridine and azopyridine osmium(ii) arene anticancer complexes. Chemical Science, Vol.3 (No.8). pp. 2485-2494.
Permanent WRAP url:
http://wrap.warwick.ac.uk/53174

Publisher's statement:
http://dx.doi.org/10.1039/C2SC20220D
A note on versions:
The version presented here may differ from the published version or, version of record, if you wish to cite this item you are advised to consult the publisher's version. Please see the 'permanent WRAP url' above for details on accessing the published version and note that access may require a subscription.

For more information, please contact the WRAP Team at: wrap@warwick.ac.uk
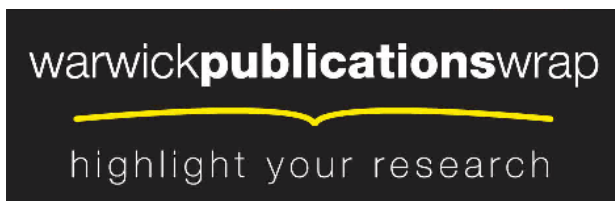
warwick**publications**wrap
highlight your research

http://go.warwick.ac.uk/lib-publications

The contrasting chemical reactivity of potent isoelectronic iminopyridine and azopyridine osmium(II) arene anticancer complexes

Ying Fu, María J. Romero, Abraha Habtemariam, Michael E. Snowden, Lijiang Song, Guy J. Clarkson, Bushra Qamar, Ana M. Pizarro, Patrick R. Unwin and Peter J. Sadler*

A wide variety of steric and electronic features can be incorporated into transition metal coordination complexes, offering the prospect of rationally-designed therapeutic agents with novel mechanisms of action. Here we compare the chemical reactivity and anticancer activity of organometallic Os^{II} complexes $[Os(\eta^6\text{-arene})(XY)Z]PF_6$ where arene = *p*-cymene or biphenyl, XY = *N,N'*-chelated phenyliminopyridine or phenylazopyridine derivatives, and Z = Cl or I. The X-ray crystal structure of $[Os(\eta^6\text{-}p\text{-cym})(Impy\text{-}OH)I]PF_6 \cdot 0.5CH_2Cl_2 \cdot H_2O$ (Impy-OH = 4-[(2-pyridinylmethylene)amino]-phenol) is reported. Like the azopyridine complexes we reported recently (*Dalton Trans.* **2011**, *40, 10553-10562*), some iminopyridine complexes are also potently active towards cancer cells (nanomolar IC_{50} values). However we show that, unlike the azopyridine complexes, the iminopyridine complexes can undergo aquation, bind to the nucleobase guanine, and oxidize coenzyme nicotine adenine dinucleotide (NADH). We report the first detection of an Os-hydride adduct in aqueous solution by ^1H NMR (-4.2 ppm). Active iminopyridine complexes induced a dramatic increase in the levels of reactive oxygen species (ROS) in A549 lung cancer cells. The anticancer activity may therefore involve interference in the redox signalling pathways in cancer cells by a novel mechanism.

Introduction

Transition metal coordination complexes offer a variety of electronic and structural features for the design of therapeutic agents, including the choice of the metal and its oxidation state, the number and types of coordinated ligands, and their coordination geometries.[1-9] The heavier, third-row (5d) transition elements in particular tend to exhibit slow ligand exchange kinetics and so might reach biological target sites with at least some of the initial ligands still bound. Organometallic arene and cyclopentadienyl complexes are attractive[10-13] since their potential amphiphilicity can be beneficial for drug transport and target recognition. Subtle changes in structure can lead to dramatic changes in chemical reactivity and biological activity. For example, certain inert *N,N'*-chelated half-sandwich organometallic iodido Os^{II} arene azopyridine complexes exhibit potent *in vitro* and *in vivo* anticancer activity.[14, 15] Their mechanism of action is different from that of N,O-chelated Os^{II} arene picolinate complexes which can hydrolyze and then bind to DNA bases,[16] with DNA being a likely target, as it is for cisplatin.[17,18] In contrast, with the strong π-acceptor azopyridine present, Ru^{II} arene complexes with iodide as the monodentate ligand are relatively inert towards substitution reactions and appear to be activated by redox reactions, for example with glutathione.[19]

Other than glutathione, the couple NADH and oxidized nicotinamide adenine dinucleotide (NAD^+) is also an important part of the cellular redox balance system.[20] Under physiological conditions, the ratio of $[NADH]/[NAD^+]$ in cells is low.[21] The cellular concentration of free NADH is in the nanomolar range,[21] which makes it a potential and sensitive target for anticancer drugs.

Early work by Steckhan[22] and Fish[23] demonstrated an efficient process for the regeneration of NADH from NAD^+ using formate as an hydride source and rhodium catalysts. Similarly we have shown that ruthenium arene anticancer complexes can reduce NAD^+ regioselectively to NADH through transfer hydrogenation.[24] Recent studies have shown that both organometallic Ru^{II} arene complexes and Ir^{III} Cp* complexes can oxidize NADH to NAD^+.[25-27] However, there are no reports of osmium complexes as transfer hydrogenation catalysts in aqueous solution.

There are some intriguing differences between the chemical properties of organometallic Ru^{II} and Os^{II} arene complexes even though their three-dimensional structures can be almost identical.[28] For example, complexes of Os^{II} (a low-spin 5d^6 metal ion) are often more inert,[16, 29] and aqua adducts of Os^{II} arenes are more acidic.[16] Several organometallic osmium anticancer complexes have been designed based on their ruthenium analogues.[30-32] Studies of both Ru^{II} and Os^{II} azopyridine anticancer complexes have been reported. However, no anticancer studies of ruthenium arene complexes with iminopyridine ligands have been reported. Osmium(II) arene phenylazopyridine complexes exhibit anticancer activity in the nanomolar range *in vitro*.[14] Moreover the complex $([Os(\eta^6\text{-}p\text{-cym})(Azpy\text{-}NMe_2)I]PF_6$ (**FY026**) is active against

coloreactal cancer *in vivo* and has low toxicity.[15] The exploration of bioisosterism provides a useful approach to the study of the anticancer activity[33] of osmium arene complexes. Here we compare the chemical reactivity and biological activity of Os[II] arene azopyridine (N=N) complexes with isoelectronic iminopyridine (HC=N) complexes. Anticancer activity has been studied in A2780 ovarian cancer cells as well as in the NCI 60-cell line panel. To investigate possible redox mechanisms, the production of ROS in lung cancer cells was studied as well as the influence of combined administration with the glutathione synthase inhibitor L-buthionine-sulfoximine (L-BSO).[34] Attempts are made to correlate biological activity with chemical reactivity through studies of aquation, binding to the nucleobase guanine, and redox reactions with glutathione and NADH. The data suggest that these osmium arene complexes possess novel mechanisms of action that can be finely tuned through the choice of the ligands.

Results
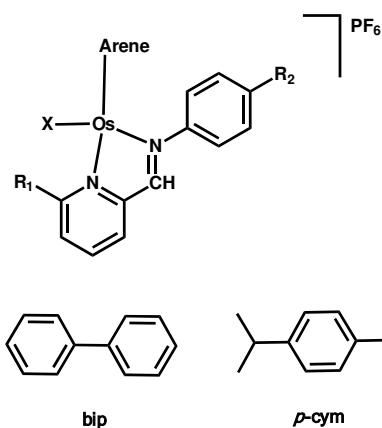
Complex	Arene	R_1	R_2	X	Chelating ligand
1	bip	H	H	I	Impy
2	*p*-cym	H	H	I	Impy
3	bip	H	OH	I	Impy-OH
4	*p*-cym	H	OH	I	Impy-OH
5	bip	H	NMe₂	I	Impy-NMe₂
6	*p*-cym	H	NMe₂	I	Impy-NMe₂
7	bip	OMe	NMe₂	I	OMe-Impy-NMe₂
8	*p*-cym	OMe	NMe₂	I	OMe-Impy-NMe₂
9	bip	H	H	Cl	Impy
10	*p*-cym	H	H	Cl	Impy
11	bip	H	OH	Cl	Impy-OH
12	*p*-cym	H	OH	Cl	Impy-OH
13	bip	H	NMe₂	Cl	Impy-NMe₂
14	*p*-cym	H	NMe₂	Cl	Impy-NMe₂
15	bip	OMe	NMe₂	Cl	OMe-Impy-NMe₂
16	*p*-cym	OMe	NMe₂	Cl	OMe-Impy-NMe₂

Chart 1 Osmium (II) arene iminopyridine complexes synthesized and studied in this work.

Synthesis and characterization

Sixteen osmium(II) arene iminopyridine complexes (Chart 1) of general formula [Os(η⁶-arene)(R₁-Impy-R₂)X]PF₆ [arene = biphenyl (bip) or *p*-cymene (*p*-cym); X = Cl or I] containing different chelating iminopyridine ligands [Impy (R₁= R₂= H), Impy-OH (R₁= H, R₂= OH), Impy-NMe₂ (R₁= H, R₂= NMe₂) and OMe-Impy-NMe₂ (R₁= OMe, R₂= NMe₂)] were synthesized. The general method involved stirring an osmium dimer and the appropriate chelating iminopyridine ligand (synthesized following a literature method)[35] in a methanol solution, similar to that reported previously for the synthesis of the azopyridine analogues.[14] In general, the iminopyridine complexes were obtained in good yields and were well characterized by ¹H-NMR spectroscopy, mass spectrometry and CHN elemental analysis (for details see ESI).

Half-sandwich organometallic arene complexes containing an unsymmetrical chelating ligand and a monodentate ligand, are chiral. ¹H NMR spectra recorded before and after adding the chiral anionic shift-reagent Δ–trisphat to a solution of complex **14** in CDCl₃, 298 K, showed a splitting of the peaks (Figure S1), indicating the presence of two enantiomers in ca. 1:1 ratio, consistent with a previous report on osmium/ruthenium arene picolinamide anticancer complexes.[17] No attempt was made to separate the enantiomers, although the chirality at the metal centre may affect anticancer activity if the biological target is chiral.

Recrystallization of [Os(η⁶-*p*-cym)(Impy-OH)I]PF₆ (**4**) from DCM/methanol afforded purple single crystals corresponding to **4**·0.5CH₂Cl₂·H₂O suitable for X-ray diffraction (Figure 1). Crystallographic data are listed in Table S1 and selected bond lengths and angles in Table S2. The asymmetric unit contains two crystallographically independent cations [Os(η⁶-*p*-cym)(Impy-OH)I]⁺ comprising of either enantiomer.
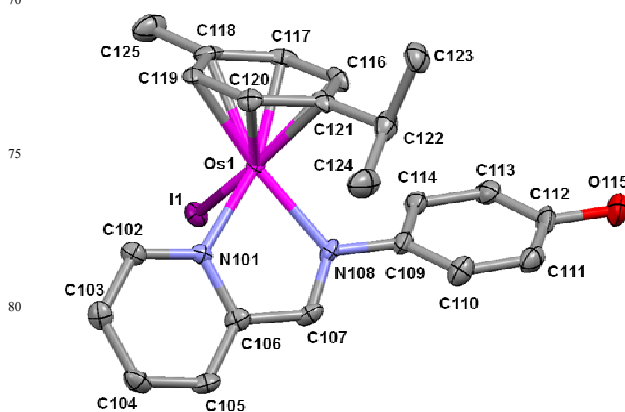
Fig. 1 X-ray structure of the cation [Os(η⁶-*p*-cym)(Impy-OH)I]⁺ in crystals of **4**·0.5CH₂Cl₂·H₂O showing the atom numbering scheme. The thermal ellipsoids are drawn at 50% probability. The hydrogen atoms, counterion (PF₆⁻), and solvent molecules have been omitted for clarity.

In addition, the two enantiomers are partially solvated by one dichloromethane and two water molecules in the asymmetric unit. The osmium complex shows a pseudo-octahedral "piano-stool" structure with the *p*-cymene ligand π-bonded to the metal ion and

the Impy-OH chelating ligand coordinated through the pyridine and imine nitrogen atoms. The imine bond adopts an *E* conformation, minimising the steric hindrance arising from the bulky phenol group. The coordination sphere of the Os^{II} ion is completed by a terminal monodentate iodide. The Os–N (2.077(4)-2.087(4) Å), Os–I (2.7091(4) Å, 2.7247(4) Å) and Os–arene centroid bond lengths (1.6845(2) Å, 1.6962(2) Å) in this complex are similar to those of the osmium analogues previously reported.[16] The crystal structure of **4**·0.5CH$_2$Cl$_2$·H$_2$O shows differences from the reported crystal structure of [Os(η^6-bip)(Azpy-O)I]·0.5H$_2$O.[14] In complex **4**·0.5CH$_2$Cl$_2$·H$_2$O there is no deprotonation of the hydroxyl group on the chelating ligand which allows both molecules to establish an hydrogen bond between the phenolic OH group of the iminopyridine ligand and a water molecule [O115-H11H···O400 1.84 Å, O215-H21H···O300 1.89 Å] as shown in Figure S2.

Aquation, pK$_a$ of aqua complexes and binding to 9-ethylguanine

The possible activation of these complexes by aquation and their interaction with 9-ethylguanine (9-EtG), a model DNA nucleobase, were studied by ^{1}H NMR spectroscopy. It was found that the osmium iminopyridine complexes [Os(η^6-*p*-cym)(Impy-NMe$_2$)I]PF$_6$ (**6**) and [Os(η^6-*p*-cym)(Impy-NMe$_2$)Cl]PF$_6$ (**14**), can undergo aquation. After incubation of the samples at 310 K for 24 h in D$_2$O, the extent of aquation reached 50% and 99%, respectively. The formation of the aqua product (**14A**) was confirmed by the presence of new signals in the ^{1}H NMR spectra shifted with respect to the signals observed for **14** (Figure S3). These signals were confirmed as corresponding to the aqua adduct after repeating the experiment in the presence of 500 mM NaCl where only one set of signals for the chlorido complex was observed.
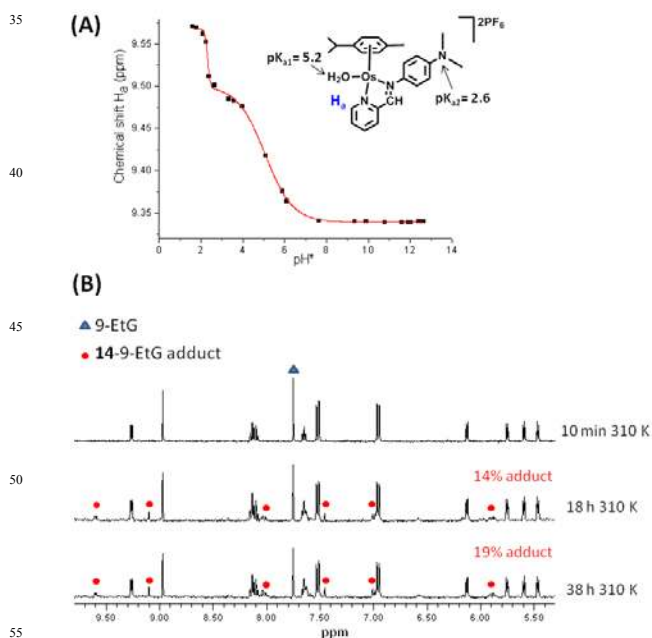

Fig. 2 (A) Dependence of the ^{1}H NMR chemical shift of the pyridine ortho proton H$_a$ on pH* in complex **14A.** The line represents a computer best fit giving pK$_a^*$ values of 5.1 (pK$_a$ 5.2)

for the coordinated water and 2.3 (pK$_a$ 2.6) for the dimethylamine substituent; **(B)** Reaction of the hydroxido complex **14A** (1 mM) with 9-ethylguanine (2 mM, 2 mol equiv) in 10%D$_2$O/90%H$_2$O phosphate buffer, pH* 7.4, followed by ^{1}H NMR. The spectra were recorded 10 min after preparing the mixture and after incubation for 18 h and 38 h at 310 K.

The pK$_a$ value of the aqua adduct (**14A**) was determined by ^{1}H NMR spectroscopy (Figure 2A). The chemical shifts of the ^{1}H NMR signals gradually shifted upfield with increase in pH* from c.a. pH* 1.5 to 13. A plot of the chemical shift of the pyridine proton H$_a$ against pH* was fitted to the Henderson-Hasselbalch equation, giving a pK$_a$ value of 5.2.[36] The low pK$_a$ value obtained for the aqua adduct suggests that the hydroxido adduct will be the predominant species under physiological conditions. The pK$_a$ value of 2.6 for the dimethylamine substituent on the iminopyridine chelating ligand Impy-NMe$_2$ is the first reported pK$_a$ of an NMe$_2$ substituent in this type of ligand bound to metal (Figure 2A).

To study the potential for DNA binding, the reaction of **14A** with 9-EtG in 0.1 M phosphate buffer (10%D$_2$O/90%H$_2$O, pH* 7.4) was monitored over various time intervals by ^{1}H NMR spectroscopy after incubation of the solution at 310 K. 9-EtG binding was confirmed by the appearance of a new set of peaks assignable to a **14**-9-EtG adduct shifted downfield in comparison to the peaks of **14A**, while the signals corresponding to coordinated 9-EtG shifted upfield with respect to the free nucleobase. The extent of binding reached only 14% after 18 h and increased only slightly to 19% after another 20 h of incubation at 310 K (Figure 2B).

Anticancer Activity

The activity of all sixteen osmium arene iminopyridine complexes towards the A2780 human ovarian cancer cell line was determined and of selected complexes towards the A549 human lung cancer cell line (Table 1). They exhibit a broad range of anticancer activity with IC$_{50}$ values (the concentration that inhibits cell growth by 50%) towards A2780 cells ranging from 0.14 µM for [Os(η^6-bip)(Impy-NMe$_2$)I]PF$_6$ (**5**) to 35.5 µM for [Os(η^6-*p*-cym)(OMe-Impy-NMe$_2$)I]PF$_6$ (**8**) (Table 1A). When the ortho -OMe substituent on the pyridine ring in **8** was replaced by H in [Os(η^6-*p*-cym)(Impy-NMe$_2$)I]PF$_6$ (**6**), the anticancer activity increased 44-fold (IC$_{50}$ decreased from 35.5 µM to 0.80 µM). This trend was also observed when biphenyl is the arene and the monodentate ligand is chloride where a 35-fold increase in anticancer activity was observed. Anticancer efficacy was also observed towards A549 cells. A significant enhancement in activity was obtained by combination treatment with L-buthionine-sulfoximine (L-BSO), a specific inhibitor of γ-glutamylcysteine synthetase (Table 1B). L-BSO depletes intracellular glutathione, which plays an important role in the maintenance of the redox balance in cancer cells.

Table 1 Anticancer activity *in vitro* towards (A) A2780 human ovarian cancer cells, (B) A549 human lung cancer cells and combination treatment with 50 µM L-BSO, (C) NCI 60-cell line screening (data for 58 cell lines) of complexes **6** and **14**.

(A) A2780 Ovarian Cancer Cells

	Complex	IC_{50}(µM)
(1)	$[Os(\eta^6\text{-bip})(Impy)I]PF_6$	18.6 (±0.9)
(2)	$[Os(\eta^6\text{-}p\text{-cym})(Impy)I]PF_6$	29.4 (±5.3)
(3)	$[Os(\eta^6\text{-bip})(Impy\text{-OH})I]PF_6$	5.4 (±1.1)
(4)	$[Os(\eta^6\text{-}p\text{-cym})(Impy\text{-OH})I]PF_6$	31.8 (±3.8)
(5)	$[Os(\eta^6\text{-bip})(Impy\text{-NMe}_2)I]PF_6$	0.14 (±0.01)
(6)	$[Os(\eta^6\text{-}p\text{-cym})(Impy\text{-NMe}_2)I]PF_6$	0.80 (±0.05)
(7)	$[Os(\eta^6\text{-bip})(OMe\text{-Impy-NMe}_2)I]PF_6$	9.14 (±0.93)
(8)	$[Os(\eta^6\text{-}p\text{-cym})(Ome\text{-Impy-NMe}_2)I]PF_6$	35.5 (±3.2)
(9)	$[Os(\eta^6\text{-bip})(Impy)Cl]PF_6$	4.6 (±0.4)
(10)	$[Os(\eta^6\text{-}p\text{-cym})(Impy)Cl]PF_6$	26.2 (±2.8)
(11)	$[Os(\eta^6\text{-bip})(Impy\text{-OH})Cl]PF_6$	2.4 (±1.1)
(12)	$[Os(\eta^6\text{-}p\text{-cym})(Impy\text{-OH})Cl]PF_6$	5.5 (±0.6)
(13)	$[Os(\eta^6\text{-bip})(Impy\text{-NMe}_2)Cl]PF_6$	0.44 (±0.01)
(14)	$[Os(\eta^6\text{-}p\text{-cym})(Impy\text{-NMe}_2)Cl]PF_6$	1.50 (±0.047)
(15)	$[Os(\eta^6\text{-bip})(OMe\text{-Impy-NMe}_2)Cl]PF_6$	9.50 (±0.22)
(16)	$[Os(\eta^6\text{-}p\text{-cym})(OMe\text{-Impy-NMe}_2)Cl]PF_6$	32.9 (±1.2)
Cisplatin		1.8 (±0.1)

(B) A549 Lung Cancer Cells

Complex	IC_{50}(µM)	IC_{50}(µM) with L-BSO
3	4.55(±1.09)	1.59(±0.36)
6	3.7(±0.2)	0.7 (±0.1)
9	>100	25.88(±12.29)
10	0.9(±0.09)	NA[a]
13	2.55(±1.35)	NA[a]
14	6.65(±0.06)	2.34(±1.18)
Cisplatin	8.68(±2.11)	NA[a]

(C) NCI 60-Cell Line

Complex[b]	IC_{50}(µM)	TGI(µM)	LC_{50}(µM)
6	3.72	13.2	49
14	8.3	33.9	75.8
Cisplatin[b]	10.3	50.7	90.5

[a] NA = not acquired. [b] Data from NCI/DTP screening. **6** = NSC755639; **14** = NSC755640. Mean-graph midpoint (MG-MID) for IC_{50}, TGI and LC_{50} values of NCI all cell panels.

The potency of complexes $[Os(\eta^6\text{-}p\text{-cym})(Impy\text{-NMe}_2)I]PF_6$ (**6**) and $[Os(\eta^6\text{-}p\text{-cym})(Impy\text{-NMe}_2)Cl]PF_6$ (**14**) towards A2780 cancer cells was similar to that of the anticancer drug cisplatin and so were further screened in the human tumour 60-cell line panel of the Developmental Therapeutics Program of the National Cancer Institute (DTP of NCI), which includes nine tumour-type subpanels. The mean values of IC_{50}, TGI (the concentration which inhibits cell growth by 100 %) and LC_{50} (the concentration that kills original cells by 50 %) are listed in Table S3. Both complexes showed anticancer activity within the same range as cisplatin (Table 1C). Complexes **6** and **14** showed a broad spectrum of activity, with IC_{50} values ranging from 0.5 µM to more than 100 µM, and a particular selectivity for melanoma and breast cancer cells. The high activity towards MDA-MB-468 breast cancer cells is particularly notable, with some IC_{50} values in the nanomolar-micromolar range (0.46 µM for **6** and 2.06 µM for **14**).

Both complex **14** and cisplatin (CDDP) showed higher activity towards A549 human lung cancer cells (8.7 µM for cisplatin and 6.7 µM for **14**, Figure 3) compared to MRC-5 human fetal lung fibroblast-like cells (IC_{50} values of 16.6 µM and 51.3 µM, respectively). Hence the ratio of IC_{50} values in normal cells compared to this cancer cell line is ca. 2 for cisplatin but increases to ca. 8 for complex **14**.
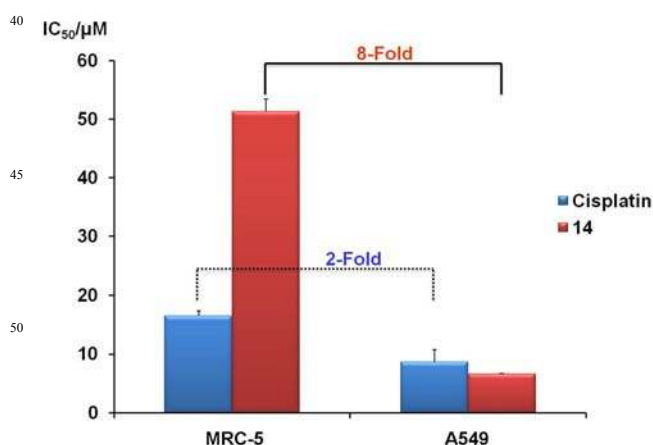

Fig. 3 *In vitro* cytotoxicity data for cisplatin and complex **14** towards A549 human lung cancer cells and MRC-5 human fetal lung fibroblast-like cells.

Induction of Reactive Oxygen Species (ROS) in Lung Cancer Cells

Os^{II} arene azopyridine complexes can increase ROS levels in cancer cells.[14] Consequently, the effect of iminopyridine complexes on cellular ROS levels was also investigated. The level of ROS induced in A549 human lung cancer cells by osmium complexes **6** and **14** was monitored using the probe 2,7-dichlorodihydrofluorescein-diacetate (DCFH-DA). This hydrolyzes to 2,7-dichlorodihydrofluorescein (DCFH) in live cells, and in turn is oxidized to 2,7-dichlorofluorescein (DCF) in the presence of ROS, exhibiting a green fluorescence.[37, 38] Using this probe, the level of general oxidative stress induced in A549 cells by **6** and **14** was determined. The accumulation of ROS during combined exposure to **6** or **14** with L-BSO was also studied.
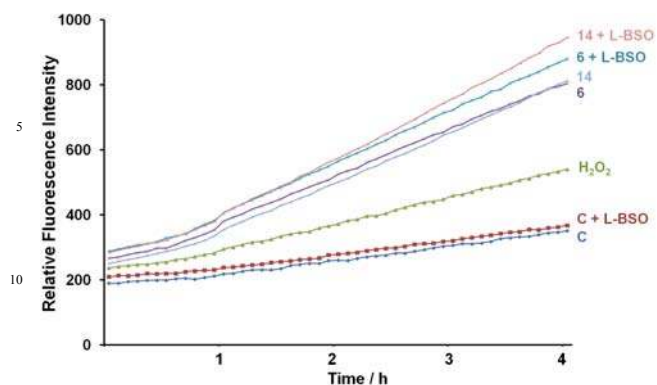
Fig. 4 Time dependence of the ROS level in A549 human lung cancer cells after treatment with **6** (4 µM), **14** (4 µM), L-BSO (50 µM), **6** or **14** combined with L-BSO (50 µM), and H_2O_2 (10 µM, positive control) during 4 h at 310 K. C= control.

In A549 cells, a relative increase in DCF fluorescence was detected over a period of 4 h after treating the cells with **6** (4 µM), **14** (4 µM), **6** (4 µM) plus L-BSO (50 µM), **14** (4 µM) plus L-BSO (50 µM) or 10 µM H_2O_2 for comparison (Figure 4). After treatment only with **6** or **14**, the ROS level increased dramatically compared to the control and even the positive control (H_2O_2, 10 µM). This level increased further in the presence of L-BSO. The further increase of ROS by the combination treatment may explain why L-BSO can enhance the cytotoxicity of complex **6** and **14** towards A549 cancer cells significantly (Table 1B). L-BSO alone at a dose of 50 µM had no significant effect on the increase of ROS (C+L-BSO, Fig.4) and the growth of A549 cancer cells, but greatly enhanced the cytotoxicity of osmium iminopyridine complexes towards A549 cancer cells.

Oxidation of NADH to NAD⁺

After observing the increase in ROS levels in cells induced by osmium iminopyridine complexes, we investigated reactions of the complexes with potential cellular reducing agents. It was found that **6** and **14** do not catalytically oxidize GSH, in contrast to their ruthenium azopyridine iodido analogues (Figure S4).[19] Since NADH/NAD⁺ is an important redox couple which maintains the redox balance in cells, reactions with NADH were also studied. Reactions of NADH with complexes **6**, **8**, **14**, **14A** and **16** were followed by ¹H NMR spectroscopy. These complexes oxidized NADH to NAD⁺ to different extents: 2.0 ± 0.2 mol equiv of NADH per mol of **14A**, 1.6 ±0.1 for **6** and **14**, and 1.2 ±0.1 for **8** and **16**, after incubation in a 10%MeOD/90%D_2O phosphate buffer solution (pH* 7.4) for 24 h at 310 K. Under these conditions the azopyridine complex [Os(η^6-*p*-cym)(Azpy-NMe₂)I]PF₆ (**FY026**) does not oxidize NADH (Figures S5 and S6). The control NADH was stable towards NAD⁺ formation under the same conditions at milimolar concentrations. Since more than one mol equiv of NADH was oxidized per mol equiv of osmium complex, this implies a catalytic mechanism. The ¹H NMR spectrum for the reaction with **14A** at 310 K (10%D_2O/90%H_2O phosphate buffer) gave a weak signal at −4.2 ppm (Figure 5) assignable to an osmium hydride adduct. This signal was detected after 27 h of reaction and was

still observable after 30 h. However, no hydride peak was detected after 45 h. This suggested that the oxidation of NADH in the presence of **14** occurs via hydride transfer to Os but the resulting Os-H adduct is unstable and decomposes.
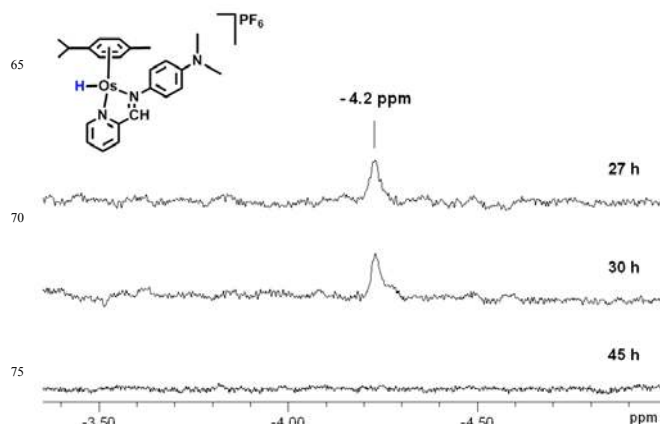

Fig. 5 Decay of the Os-H ¹H NMR peak from reaction of the hydroxido complex **14A** (2.5 mM) with 4 mol equiv of NADH in 10%D_2O/90%H_2O phosphate buffer, pH* 7.4 after different periods of incubation at 310 K.

LC-MS was also employed to analyse the products from the reaction between NADH (0.5 mM) and **14A** (0.5 mM) after incubation at 310 K for 24 h. The decrease in intensity of the peak with a retention time of ca. 11.5 min (NADH; calcd for $C_{21}H_{30}N_7O_{14}P_2$ m/z = 666.1, found m/z = 666.1) and the appearance of a new peak with a retention time of 4.8-5.2 min (NAD⁺ calcd for $C_{21}H_{28}N_7O_{14}P_2$ m/z = 664.1, found m/z = 664.1) were observed after the reaction with **14A** (Figure S7).

The reaction of the chlorido complex **14** with NADH (8 mol equiv) was monitored by UV-Vis over 18 h at 310 K in a phosphate buffer pH 7.4 (Figure 6). The kinetic experiment showed an isosbestic point at 300 nm corresponding to the oxidation of NADH to NAD⁺ and another isosbestic point at 432 nm related to the aquation of **14**, suggesting that the aquation of the chlorido complex **14** accompanies the oxidation. The formation of NAD⁺ was confirmed by a decrease in intensity of the characteristic NADH band at 338 nm and the simultaneous increase in intensity at 260 nm.
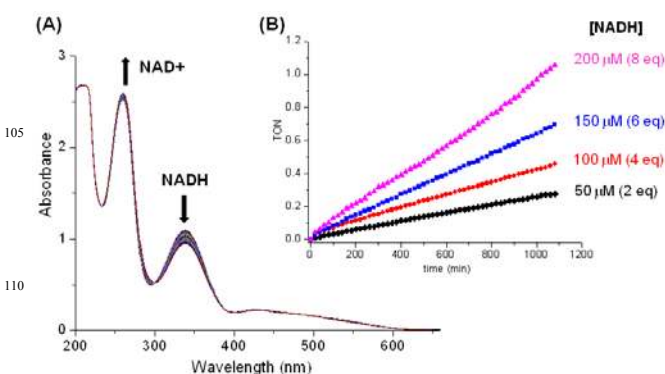

Fig. 6 (A) UV-Vis spectra for the reaction between the chlorido complex **14** (0.025 mM) and NADH (8 mol equiv) in 1 mM phosphate buffer (pH* 7.4) during 18 h at 310 K. The spectra

were recorded at intervals of 20 min. Inset: **(B)** Dependence of the turnover number (TON) of complex **14** (0.025 mM) on the mol ratio of NADH. The reaction was followed by the decrease in intensity of the NADH absorption band at 338 nm.

The dependence of the oxidative activity of **14** on the concentration of NADH in solution was studied by following the conversion of 2 and 8 mol equivalents of NADH to NAD^+ (Figure S8A) under the same conditions described above. The rate of reaction of **14** (25 μM) was similar for reactions of 2 and 8 mol equiv NADH suggesting that the formation of an initial adduct is rate-limiting. An increase in NADH concentration resulted in higher turnover numbers for complex **14** (Figure 6B).

The NAD^+/NADH ratio after 18 h was determined to be 0.14 for the reaction between **14** and 2 equiv of NADH, 0.11 for 4 equiv, 0.12 for 6 equiv and 0.13 for 8 equiv, respectively. The rate of oxidation of NADH (8 mol equiv) was the same in the presence of either 25 μM or 10 μM **14** (Figure S8B). The control solutions showed a slight decomposition of the NADH under these conditions attributable to the effect of phosphate buffer, consistent with previous reports.[39, 40]

Since the instability of the osmium hydride adduct formed by reaction with NADH might be due to protonation and liberation of H_2,[41] an attempt was made to detect H_2 as a product by gas chromatography. However, none was detected (for conditions see ESI).

The reaction between osmium complex **14** (0.1 mM) and NADH (0.4 mM) under aerobic and anaerobic (bubbling argon for 10 min) conditions was compared as monitored by ^{1}H NMR spectroscopy (18-h incubation, 310 K in 10%MeOD/90%D_2O phosphate buffer, pH^* 7.4). Under argon there was almost no conversion of NADH to NAD^+ ($3 \pm 0.5\%$ compared to $17 \pm 1\%$ in air; Figure 7). It can therefore be concluded that O_2 plays a role in the conversion of NADH to NAD^+.
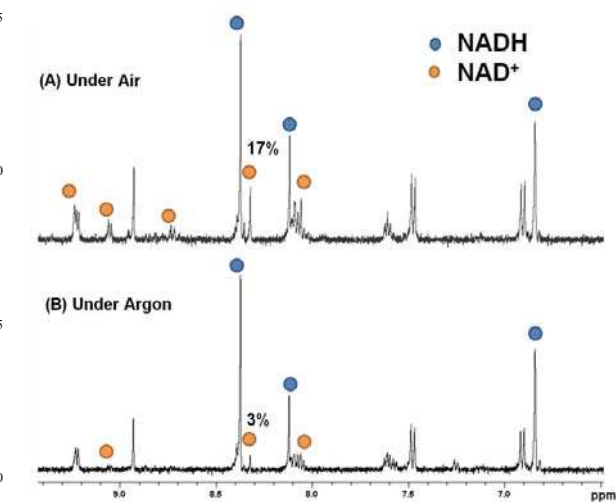

Fig. 7 ^{1}H NMR spectra for the reaction between osmium complex **14** (0.1 mM) and NADH (4 mol equiv) in 10%MeOD/90%D_2O phosphate buffer, pH^* 7.4, after 18 h of incubation at 310 K. **(A)** Under aerobic conditions, and **(B)** under argon.

After saturating a solution containing **14** (0.1 mM) and NADH (0.5 mM) with O_2 (bubbling for 10 min), the conversion of NADH to NAD^+ increased from 10% (aerobic) to 25% (O_2-saturated), whereas such saturation had little effect on a similar control solution of NADH alone (no significant NAD^+ formation after O_2 saturation and incubation for 18 h at 310 K; Figure 8).

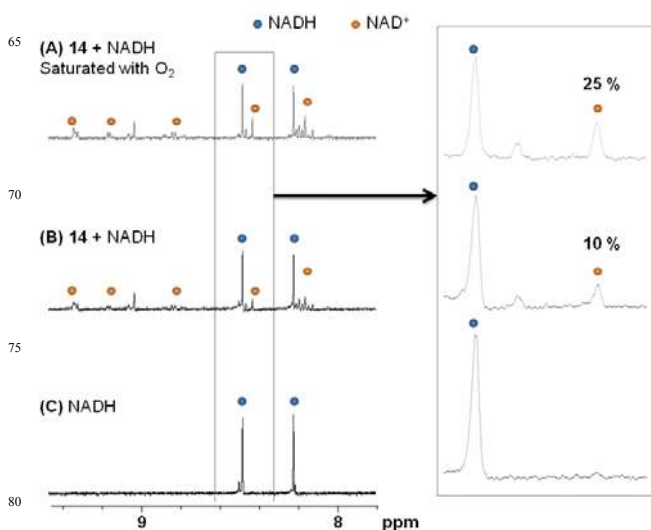**Fig. 8** ^{1}H NMR spectra for the reaction between the osmium complex **14** (0.1 mM) and NADH (5 mol equiv.) **(A)** under oxygen saturation, **(B)** in air, **(C)** NADH alone under oxygen saturation. Solvent: 10%MeOD/90%D_2O phosphate buffer, pH^* 7.4). Incubation conditions: 18 h at 310 K.

To investigate whether aquation is a necessary step for **14** to oxidize NADH to NAD^+, the reaction of **14** (0.1 mM) and NADH (0.4 mM) was carried out under three conditions: (1) without NaCl, (2) with 100 mM NaCl (3) with 500 mM NaCl. The resulting NMR spectra after 24 h incubation at 310 K are shown in Figure 9.
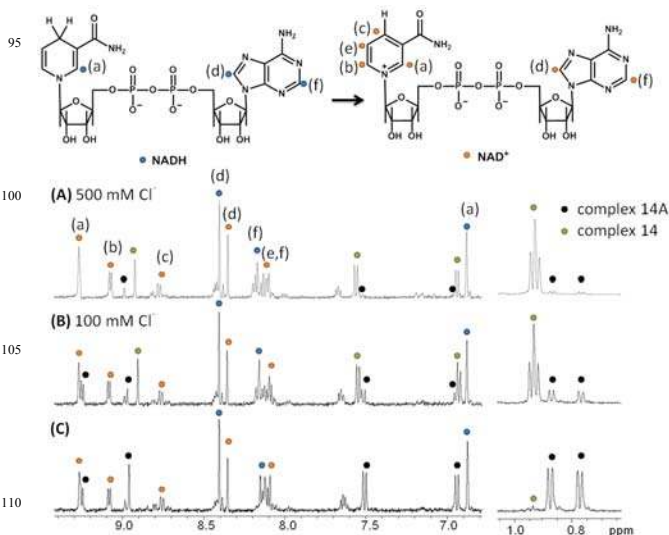

Fig. 9 Reactions of complex **14** [Os(η^6-*p*-cym)(Impy-NMe$_2$)Cl]PF$_6$ (0.1 mM) with NADH (0.4 mM) in the absence and presence of NaCl (to suppress aquation), followed by ^{1}H NMR spectroscopy. **(A)** 500 mM NaCl; **(B)** 100 mM NaCl; **(C)** no

NaCl. Solvent: 10% MeOD-d_4/90% D_2O phosphate buffer, pH[*] 7.4). ^{1}H NMR spectra were recorded 24 h after incubation at 310 K. **14A** is the aqua complex. The presence of NaCl suppresses aquation but the extent of oxidation of NADH to NAD^+ (40 ± 3%) is not affected.

The extent of aquation decreased from 99% to 11% and 1% at NaCl concentrations of 0 mM, 100 mM and 500 mM, respectively. After 24 h incubation with NADH at 310 K, the same amount of NAD^+ product (40 ± 3%) was observed for each of these three solutions (Figure 9), this result indicating that NADH can react directly with the chlorido complex.

Since complex **14** appeared to oxidize NADH by hydride transfer, we studied the effect of complex **14** on the NAD^+/NADH ratio in human ovarian A2780 cancer cells. After treatment of the cancer cells with 1.5 μM of complex **14** for 6 h (see Supporting Information), the NAD^+/NADH ratio in cell lysates increased from 2.54±0.46 to 5.44±0.26. The increase may suggest that the anticancer activity of these Os^{II} arene iminopyridine complexes can be related to their reactivity with the cellular reducing agent NADH and the consequent change in the redox status of the cancer cells.

Electrochemistry

Cyclic voltammetry studies of iodido complexes **3** and **6**, and chlorido complexes **10** and **14** together with **3** and **10** showed that these compounds underwent two irreversible electrochemical reductions in dimethylformamide with potentials ranging from –0.58 to –0.76 V for the first and –0.82 to –1 V for the second. Subtle variations in the CV morphology and forward-reverse peak separations for the different complexes suggests some small differences in heterogeneous electron transfer kinetics (Figure S9).

Discussion

Aquation and Binding to 9-Ethylguanine

The chlorido complex **14** [Os(η^6-p-cym)(Impy-NMe_2)Cl]PF_6 hydrolysed almost completely after 24 h in water at 310 K, whereas the iodido complex **6** [Os(η^6-p-cym)(Impy-NMe_2)I]PF_6 was only ca. 50% hydrolysed. This is consistent with the expected strengthening of the Os-halide bond for the heavier halides. However, both these complexes are much less stable in water than the analogous azopyridine complexes.[14]

The pK_a of the aqua adduct **14A** was determined to be 5.2, which implies that the major product of aquation at physiological pH (7.4) will be the hydroxido adduct. This may account for the low extent and slowness of binding to the nucleobase 9-ethyl guanine (only 19% after 38 h of incubation at 310K, Figure 2), since Os-OH bonds are expected to be much less reactive than Os-OH_2 bonds. We chose to study guanine as the nucleobase since G N7 is the most electron-dense site on DNA and is a known target for platinum anticancer drugs.[42]

The findings for guanine binding suggest that DNA (and RNA) could be a target for osmium iminopyridine complexes, but the extent of binding of **14** to 9-EtG was much less than for the

previously reported osmium picolinate DNA-targeted complexes,[16] which suggests that other targets may be more important. The contrast between these iminopyridine complexes and their isoelectronic azopyridines analogues is quite striking. The azopyridine complexes do not readily hydrolyse and do not bind to guanine. In accordance with this, the azopyridines appear to exert their anticancer activity partly by redox mechanisms. We also investigated whether redox mechanisms are important for iminopyridine complexes (*vide infra*).

Structure-Activity Relationships (SAR) for Human Ovarian Cancer Cells

When the anticancer activity of osmium arene phenyliminopyridine complexes with various substituents on the phenyl ring is compared with their phenylazopyridine analogues, the correlation coefficient is low (Figure 10), which suggests that the mechanism of action is different for these two families of osmium anticancer complexes. For a subset of 8 of the 11 complexes however, there is a stronger correlation, Figure 10. The iminopyridine complexes bearing a biphenyl arene exhibit higher anticancer activity towards A2780 cells than their *p*-cymene analogues (Table 1, Chart 1). It seems likely that the greater hydrophobicity of the biphenyl complexes enhances cell uptake, although intercalation into DNA may also contribute if DNA is a target.[43]
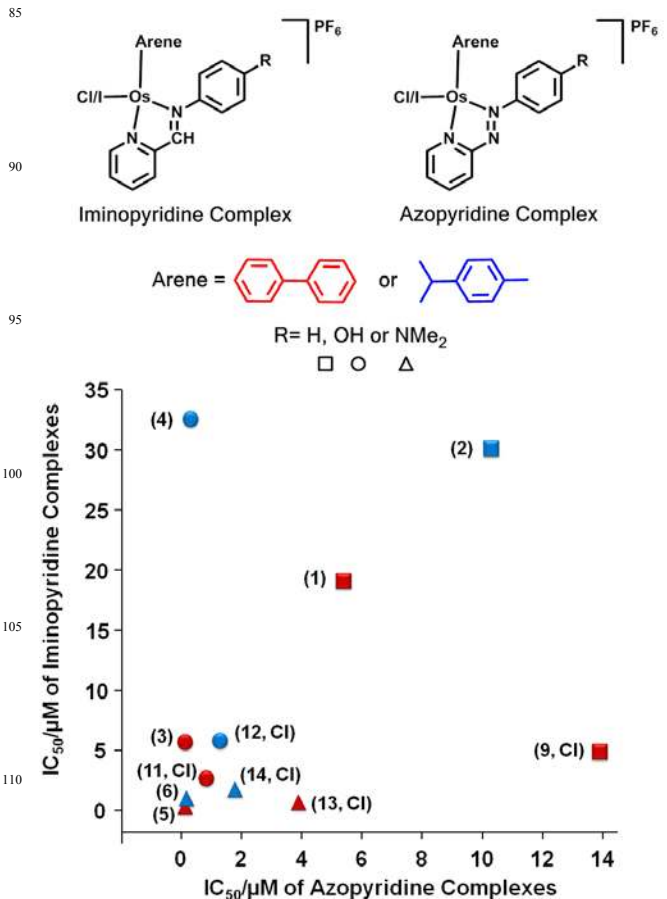

Fig. 10 Correlations of the IC_{50} values of osmium arene iminopyridine complexes with their azopyridine analogues. The

numbers in brackets refer to iminopyridine complexes (see Chart 1). Complexes with biphenyl arene (red) and *para*-cymene (blue) arene are labelled with different colours; chlorido complexes are indicated by Cl in the brackets; different substituents on the chelating ligands are designated using different shapes: R= H (square), R= OH (circle) and R= NMe$_2$ (triangle). Overall the correlation is poor (R^2= 0.0673) although if outliers **4**, **9** and **13** are ignored, then there is a reasonable correlation for the remaining 8 complexes (R^2= 0.9395).

In general, the chlorido iminopyridine complexes are as active or more active than their iodido analogues. This contrasts with the azopyridine series for which the opposite is true, except for those with a –NMe$_2$ electron-donating substituent in the phenyl ring of the phenyliminopyridine ligand. For the inert azopyridine complexes, addition of an ortho substituent such as CF$_3$ or Cl on the pyridine ring maintained or increased the anticancer activity. However, in the present case, ortho functionalization of the pyridine ring with a methoxy group decreased the anticancer activity significantly (Table 1). Unlike the azopyridine complexes, the Os-Cl/I bond is reactive in iminopyridine complexes and an ortho substituent may hinder the reactivity. Substitution reactions at the osmium centre may therefore be important in the mechanism of action of iminopyridine complexes.

Additionally, it is notable that **6** and **14** are more potent anticancer complexes than previously-reported ruthenium and osmium arene complexes which bind more strongly to DNA bases and appear to have DNA as a major target.[16, 44] Redox mediated mechanisms of activity may be more effective since they can affect multi-specific targets in cells.

Accumulation of ROS in Cancer Cells

ROS are highly reactive O$_2$ metabolites that include superoxide radicals (O$_2^-\cdot$), hydrogen peroxide (H$_2$O$_2$) and hydroxyl radicals (OH·).[45] Because cancer cells have increased ROS levels compared to normal cells, this difference can be exploited as a biochemical basis for therapeutic selectivity.[46, 47] Increased ROS levels in cancer cells can reach a threshold and induce cell death but such increases can be tolerated by normal cells.[30] This may explain why complex **14** is 8-fold more cytotoxic towards A549 human lung cancer cells compared to normal human fetal lung fibroblast-like MRC-5 cells (Fig. 3). Although ROS are generally believed to be toxic to cells, they act as a 'double-edged sword' for the proliferation of cells. When the ROS level in cells is up-regulated on a small scale, ROS may contribute to the proliferation; if the ROS level is raised further, it can cause DNA damage which will induce cell cycle arrest and apoptosis.[48] Therefore selectivity to cancer cells rather than normal cells can be achieved by increasing the ROS levels because the basal ROS levels in cancer cells are higher than in normal cells. These increases in ROS levels provide a basis for a strategy involving combination treatment of **6** or **14** with the glutathione synthesis inhibitor buthionine sulfoximine (L-BSO), Fig. 4.

Because the GSH concentration is 100-10,000 fold higher in cells compared to other reductants (e.g. NADH, NADPH and thioredoxin), the level of GSH usually determines the steady-state value of intracellular redox potentials.[49] However, complexes **6** and **14** do not readily oxidize GSH unlike ruthenium azopyridine analogues.[14] The half-wave reduction potentials of osmium complexes **3**, **6**, **10** and **14** in dimethylformamide of –0.58 to –0.76 V and –0.82 to –1 V are more negative than those of the ruthenium azopyridine complexes,[19] indicating that the iminopyridine complexes are more difficult to reduce, perhaps explaining why no reaction was observed with GSH (Figures S4 and S9). In contrast, novel reactions with the reduced coenzyme NADH, a stronger reducing agent than GSH, were observed.

Oxidation of NADH to NAD$^+$

Apart from a role in the generation of ROS, the facile oxidation of NADH may help to rationalize the surprisingly good anticancer activity of these Os^{II} iminopyridine complexes.

NMR, LC-MS and UV-Vis studies showed that osmium iminopyridine complexes can oxidize NADH to NAD$^+$. The reaction appears to involve the transfer of hydride from NADH to the Os centre with displacement of the halide ligand (I for **6** and **8**, and Cl for **14** and **16**) or aqua ligand. During the conversion of NADH to NAD$^+$ in the presence of **14A**, an osmium-hydride peak was detected by ^{1}H NMR at –4.2 ppm (Figure 5). This value is consistent with previous reports of Os-H adducts.[50, 51] The reported organometallic hydride osmium(II) compounds containing arene[52, 53] and/or imine ligands[54, 55] showed Os-H signals ranging from -9 ppm to -13 ppm (terminal hydride) and from -15 ppm to -20 ppm (bridging hydride). In all the reported compounds, the hydride peaks were detected for complexes in deuterated organic solvents such as CD$_2$Cl$_2$, acetone-d$_6$ or C$_6$D$_6$. The current work appears to be the first detection of an osmium(II) hydride NMR peak for an osmium hydride in an aqueous solution.[56-64] These findings suggest that osmium arene complexes can modulate the redox balance in cells by a novel mechanism.

^{1}H NMR studies show that complexes **6** and **14** are more effective in oxidising NADH than **8** and **16** after 24 h incubation at 310K (Figure S5). This may be due to the steric hindrance exerted by the methoxy substituent in the ortho-position of the iminopyridine chelating ligand for **8** and **16**. This trend is also observed for the anticancer activity of these compounds: **6** and **14** are ca. 20 times more potent than **8** and **16**. It is possible therefore that NADH oxidation is involved in the mechanism of anticancer activity of these osmium iminopyridine anticancer complexes.

A possible mechanism for the oxidation of NADH in the presence of these iminopyridine complexes involves hydride transfer to Os followed by protonation of bound hydride,[65] liberation of H$_2$, and regeneration of the aqua/hydroxido Os adduct, similar to that of Ir^{III} cyclopentadienyl complexes studied in our laboratory.[27] However, no H$_2$ was detected after the incubation of NADH with **14** or **14A** for 24 h at 310 K (100 mM phosphate buffer, pH 7.2). The presence of O$_2$ did appear to influence the course of the oxidation significantly, being inhibited under argon and enhanced by O$_2$ saturation (Figures 7 and 8). One possibility is that hydride is transferred from Os-H to O$_2$ to

form H_2O_2,[37] giving a cycle such as that shown in Scheme 1. However attempts to detect H_2O_2 production electrochemically were unsuccessful (for conditions see ESI).

Suppression of aquation of the chlorido complex **14** still led to the oxidation of NADH (Figure 9) suggesting that aquation is not an essential step in the mechanism and that hydride transfer can occur with direct chloride displacement.
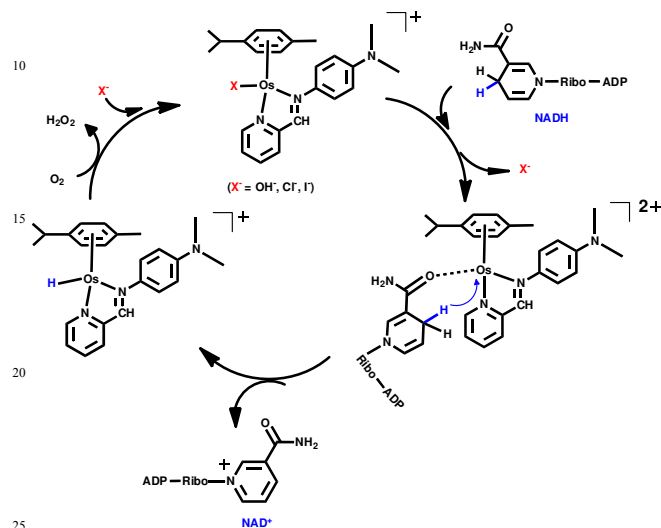
Scheme 1 A possible mechanism for the oxidation of NADH to NAD^+ catalysed by an Os^{II} arene iminopyridine complex, $X^- = OH^-$, Cl^- or I^-.[23, 27]

Conclusions

In this work, we have prepared new Os^{II} arene iminopyridine anticancer complexes to explore the effect of bioisosterism on the biological activity of our previously studied Os^{II} arene azopyridine complexes. We have contrasted the chemical reactivity and anticancer activity of isoelectronic organometallic Os^{II} complexes $[Os(\eta^6\text{-arene})(XY)Z]PF_6$ where arene = *p*-cym or bip, XY = *N,N'*-chelated phenyliminopyridine or phenylazopyridine derivatives, and Z = Cl or I. The X-ray crystal structure of $[Os(\eta^6\text{-}p\text{-cym})(Impy-OH)I]PF_6\cdot0.5CH_2Cl_2\cdot H_2O$ is reported. Some Os^{II} arene iminopyridine complexes are potently active towards cancer cells (nanomolar IC_{50} values), like the azopyridine complexes we reported recently.[66] Nevertheless, unlike the azopyridine analogues, the iminopyridine complexes hydrolyse in aqueous solution and bind to the model nucleobase 9-ethylguanine, suggesting that DNA could be a possible target for these anticancer compounds, although other targets are not excluded.

Additionally, we have found that active iminopyridine complexes induce a dramatic increase in the levels of reactive oxygen species (ROS) in A549 lung cancer cells. For this reason, we investigated the possibility that these Os^{II} complexes can be involved in biologically-relevant redox chemistry, for example with the cellular reducing agents glutathione (GSH) and reduced coenzyme nicotine adenine dinucleotide (NADH). The Os^{II} arene iminopyridine compounds followed opposite trends in redox reactivity compared to the azo analogues: the iminopyridine complexes were inert toward GSH but they could oxidize NADH to different extents depending on the substituents on the chelating ligand. A mechanism for the oxidation of NADH to NAD^+ through the formation of an Os-hydride adduct in aqueous solution detected by ^{1}H NMR (singlet at -4.2 ppm) is proposed. Furthermore, an increase in the ratio of NAD^+/NADH in human ovarian A2780 cancer cells after treatment with the chlorido complex $[Os(\eta^6\text{-}p\text{-cym})(Impy-NMe_2)Cl]PF_6$ was found.

We conclude from these studies that the anticancer activity of these osmium arene iminopyridine complexes may involve the modulation of redox pathways in cancer cells by a novel mechanism. In addition, we have shown that the rational design of the chelating ligands and structure of the Os^{II} arene complexes plays an important role in controlling the reactivity and biological behaviour of these anticancer drugs.

Table 2 Comparison between the biological and chemical behaviour of osmium(II) arene iminopyridine complexes and azopyridine complexes.

$[Os(\eta^6\text{-arene})(XY)Z]^+$ Complexes		
	XY =	
Property	**Iminopyridine**	**Azopyridine**
Activity to A2780 cells	Nanomolar	Nanomolar
Increase in ROS	Yes	Yes
Oxidation of GSH	No	No
Oxidation of NADH	Yes	No
Aquation	Yes	No
Binding to 9-EtG	Yes	No

Acknowledgements

Notes and references

Department of Chemistry, University of Warwick, Gibbet Hill Road, Coventry CV4 7AL, UK. Tel: +44-2476523818; Fax: +44-2476523819. Email: P.J.Sadler@warwick.ac.uk

† Electronic Supplementary Information (ESI) available: Experimental Section (synthesis and characterisation of complexes), Methods (electrochemistry, LC-MS, GC, X-ray crystallography, Cell culture and IC_{50} determinations, ROS detection, $NAD^+/NADH$ ratio in cells), Instrumentation, Tables S1 and S2 of crystallographic data, Table S3 of NCI 60-cell line anticancer data, and Figures S1-S9. CCDC reference number 867420. See DOI: 10.1039/b000000x/.

1. C. G. Hartinger, S. Zorbas-Seifried, M. A. Jakupec, B. Kynast, H. Zorbas and B. K. Keppler, *J. Inorg. Biochem.*, 2006, **100**, 891-904.
2. M. Galanski, V. B. Arion, M. A. Jakupec and B. K. Keppler, *Curr. Pharm. Des.*, 2003, **9**, 2078-2089.
3. C. G. Hartinger and P. J. Dyson, *Chem. Soc. Rev.*, 2009, **38**, 391-401.
4. U. Schatzschneider and N. Metzler-Nolte, *Angew. Chem., Int. Ed.*, 2006, **45**, 1504-1507.
5. G. Gasser, I. Ott and N. Metzler-Nolte, *J. Med. Chem.*, 2010, **54**, 3-25.
6. G. I. Pascu, A. C. G. Hotze, C. Sanchez-Cano, B. M. Kariuki and M. J. Hannon, *Angew. Chem., Int. Ed.*, 2007, **119**, 4452-4456.
7. E. Hillard, A. Vessières, L. Thouin, G. Jaouen and C. Amatore, *Angew. Chem., Int. Ed.*, 2006, **45**, 285-290.
8. G. Sava, A. Bergamo, S. Zorzet, B. Gava, C. Casarsa, M. Cocchietto, A. Furlani, V. Scarcia, B. Serli, E. Iengo, E. Alessio and G. Mestroni, *Eur. J. Cancer*, 2002, **38**, 427-435.
9. W.-X. Ni, W.-L. Man, M. T.-W. Cheung, R. W.-Y. Sun, Y.-L. Shu, Y.-W. Lam, C.-M. Che and T.-C. Lau, *Chem. Commun.*, 2011, **47**, 2140-2142.
10. O. Novakova, J. Kasparkova, O. Vrana, P. M. van Vliet, J. Reedijk and V. Brabec, *Biochemistry*, 1995, **34**, 12369-12378.
11. P. Annen, S. Schildberg and W. S. Sheldrick, *Inorg. Chim. Acta*, 2000, **307**, 115-124.
12. O. R. Allen, L. Croll, A. L. Gott, R. J. Knox and P. C. McGowan, *Organometallics*, 2003, **23**, 288-292.
13. D. R. van Staveren and N. Metzler-Nolte, *Chem. Rev.*, 2004, **104**, 5931-5986.
14. Y. Fu, A. Habtemariam, A. M. Pizarro, S. H. van Rijt, D. J. Healey, P. A. Cooper, S. D. Shnyder, G. J. Clarkson and P. J. Sadler, *J. Med. Chem.*, 2010, **53**, 8192-8196.
15. S. D. Shnyder, Y. Fu, A. Habtemariam, S. H. van Rijt, P. A. Cooper, P. M. Loadman and P. J. Sadler, *Med. Chem. Commun.*, 2011, **2**, 666-668.
16. A. F. A. Peacock, S. Parsons and P. J. Sadler, *J. Am. Chem. Soc.*, 2007, **129**, 3348-3357.
17. S. H. van Rijt, A. J. Hebden, T. Amaresekera, R. J. Deeth, G. J. Clarkson, S. Parsons, P. C. McGowan and P. J. Sadler, *J. Med. Chem.*, 2009, **52**, 7753-7764.
18. H. Kostrhunova, J. Florian, O. Novakova, A. F. A. Peacock, P. J. Sadler and V. Brabec, *J. Med. Chem.*, 2008, **51**, 3635-3643.
19. S. J. Dougan, A. Habtemariam, S. E. McHale, S. Parsons and P. J. Sadler, *Proc. Natl. Acad. Sci. U. S. A.* 2008, **105**, 11628-11633.
20. W. Ying, *Antioxidants & Redox Signaling*, 2008, **10**, 179-206.
21. Q. Zhang, D. W. Piston and R. H. Goodman, *Science*, 2002, **295**, 1895-1897.
22. E. Steckhan, S. Herrmann, R. Ruppert, E. Dietz, M. Frede and E. Spika, *Organometallics*, 1991, **10**, 1568-1577.
23. H. C. Lo, C. Leiva, O. Buriez, J. B. Kerr, M. M. Olmstead and R. H. Fish, *Inorg. Chem.*, 2001, **40**, 6705-6716.
24. Y. Yan, M. Melchart, A. Habtemariam, A. Peacock and P. Sadler, *J. Biol. Inorg. Chem.*, 2006, **11**, 483-488.
25. Z. Liu, A. Habtemariam, J. J. Soldevila, A. M. Pizarro, P. J. Sadler, PCT Int. Appl. 2011, 88p, WO/2011/148124.
26. Y. Maenaka, T. Suenobu and S. Fukuzumi, *J. Am. Chem. Soc.*, 2012, **134**, 367-374.
27. S. Betanzos-Lara, Z. Liu, A. Habtemariam, A. M. Pizarro, B. Qamar and P. J. Sadler, *Angew. Chem., Int. Ed.*, 2012, **51**, 3897-3900.
28. J. Maksimoska, D. S. Williams, G. E. Atilla-Gokcumen, K. S. M. Smalley, P. J. Carroll, R. D. Webster, P. Filippakopoulos, S. Knapp, M. Herlyn and E. Meggers, *Chem.-Eur. J.*, 2008, **14**, 4816-4822.
29. A. Dorcier, W. H. Ang, S. Bolaño, L. Gonsalvi, L. Juillerat-Jeannerat, G. Laurenczy, M. Peruzzini, A. D. Phillips, F. Zanobini and P. J. Dyson, *Organometallics*, 2006, **25**, 4090-4096.
30. A. F. A. Peacock, A. Habtemariam, S. A. Moggach, A. Prescimone, S. Parsons and P. J. Sadler, *Inorg. Chem.*, 2007, **46**, 4049-4059.
31. G. E. Büchel, I. N. Stepanenko, M. Hejl, M. A. Jakupec, B. K. Keppler and V. B. Arion, *Inorg. Chem.*, 2011, **50**, 7690-7697.
32. B. Cebrián-Losantos, A. A. Krokhin, I. N. Stepanenko, R. Eichinger, M. A. Jakupec, V. B. Arion and B. K. Keppler, *Inorg. Chem.*, 2007, **46**, 5023-5033.
33. Y. C. Martin, *J. Med. Chem.*, 1981, **24**, 229-237.
34. U. Vanhoefer, S. Cao, H. Minderman, K. Toth, B. S. Skenderis, M. L. Slovak and Y. M. Rustum, *Clin. Cancer Res.*, 1996, **2**, 1961-1968.
35. S. S. Hindo, A. M. Mancino, J. J. Braymer, Y. Liu, S. Vivekanandan, A. Ramamoorthy and M. H. Lim, *J. Am. Chem. Soc.*, 2009, **131**, 16663-16665.
36. A. Krezel and W. Bal, *J. Inorg. Biochem.*, 2004, **98**, 161-166.
37. H. Wang and J. A. Joseph, *Free Radical Biol. Med.* 1999, **27**, 612-616.
38. A. Gomes, E. Fernandes and J. L. F. C. Lima, *J. Biochem. Biophys. Methods*, 2005, **65**, 45-80.
39. J. Wu, L. Wu and J. Knight, *Clin. Chem.*, 1986, **32**, 314-319.
40. R. M. Burton and N. O. Kaplan, *Arch. Biochem. Biophys.*, 1963, **101**, 139-149.
41. C. Creutz, M. H. Chou, H. Hou and J. T. Muckerman, *Inorg. Chem.*, 2010, **49**, 9809-9822.
42. B. Song, J. Zhao, R. Griesser, C. Meiser, H. Sigel and B. Lippert, *Chem.-Eur. J.*, 1999, **5**, 2374-2387.
43. H.-K. Liu, S. J. Berners-Price, F. Wang, J. A. Parkinson, J. Xu, J. Bella and P. J. Sadler, *Angew. Chem., Int. Ed.*, 2006, **118**, 8333-8336.
44. H.-K. Liu and P. J. Sadler, *Acc. Chem. Res.*, 2011, **44**, 349-359.
45. V. J. Thannickal and B. L. Fanburg, *Am. J. Physiol. Lung Cell Mol. Physiol.*, 2000, **279**, L1005-L1028.
46. E. Hileman, J. Liu, M. Albitar, M. Keating and P. Huang, *Cancer Chemother. Pharmacol.*, 2004, **53**, 209-219.
47. J. Wang and J. Yi, *Cancer Biol. Ther.*, 2008, **7**, 1875-1884.
48. B. Halliwell, *Biochem. J.*, 2007, **401**, 1-11.
49. F. Q. Schafer and G. R. Buettner, *Free Radical Biol. Med.*, 2001, **30**, 1191-1212.
50. T. Bolaño, R. Castarlenas, M. A. Esteruelas, F. J. Modrego and E. Oñate, *J. Am. Chem. Soc.*, 2005, **127**, 11184-11195.
51. A. V. Marchenko, H. Gerard, O. Eisenstein and K. G. Caulton, *New J. Chem.*, 2001, **25**, 1244-1255.
52. S. Stahl and H. Werner, *Organometallics*, 1990, **9**, 1876-1881.
53. J. P.-K. Lau and W.-T. Wong, *Dalton Trans.*, 2005, 2579-2587.
54. J. A. Cabeza, I. del Río, F. Grepioni and V. Riera, *Organometallics*, 2000, **19**, 4643-4646.
55. S. Aime, E. Diana, R. Gobetto, M. Milanesio, E. Valls and D. Viterbo, *Organometallics*, 2001, **21**, 50-57.
56. C. L. Gross and G. S. Girolami, *Organometallics*, 2006, **26**, 160-166.

57. R. Castro-Rodrigo, M. A. Esteruelas, A. M. López and E. Oñate, *Organometallics*, 2008, **27**, 3547-3555.
58. M. A. Esteruelas, F. J. Fernández-Alvarez, A. M. López, M. Mora and E. Oñate, *J. Am. Chem. Soc.*, 2010, **132**, 5600-5601.
59. T.-Y. Cheng and R. M. Bullock, *Organometallics*, 2002, **21**, 2325-2331.
60. M. A. Esteruelas, A. M. López, E. Oñate and E. Royo, *Organometallics*, 2004, **23**, 3021-3030.
61. M. A. Esteruelas and A. M. López, *Organometallics*, 2005, **24**, 3584-3613.
62. J. Zhang, D. C. Grills, K.-W. Huang, E. Fujita and R. M. Bullock, *J. Am. Chem. Soc.*, 2005, **127**, 15684-15685.
63. C. A. Bayse, M. Couty and M. B. Hall, *J. Am. Chem. Soc.*, 1996, **118**, 8916-8919.
64. C. L. Gross and G. S. Girolami, *Organometallics*, 1996, **15**, 5359-5367.
65. H. F. Haarman, F. R. Bregman, P. W. N. M. van Leeuwen and K. Vrieze, *Organometallics*, 1997, **16**, 979-985.
66. Y. Fu, A. Habtemariam, A. M. B. H. Basri, D. Braddick, G. J. Clarkson and P. J. Sadler, *Dalton Trans.*, 2011, **40**, 10553-10562.